



Synthesis, characterization and reactivity of vanadium, chromium, and manganese PNP pincer complexes

Matthias Mastalir^a, Mathias Glatz^a, Berthold Stöger^b, Matthias Weil^b, Ernst Pittenauer^b, Günter Allmaier^b, Karl Kirchner^{a,*}

^a Institute of Applied Synthetic Chemistry, Vienna University of Technology, Getreidemarkt 9, A-1060 Vienna, Austria

^b Institute of Chemical Technologies and Analytics, Vienna University of Technology, Getreidemarkt 9, A-1060 Vienna, Austria

ARTICLE INFO

Article history:

Received 28 January 2016

Accepted 29 February 2016

Available online xxxx

Keywords:

Vanadium

Chromium

Manganese

Pincer ligands

Homo coupling

ABSTRACT

The synthesis of a series of vanadium, chromium, and manganese PNP complexes of the types $[M(PNP)Cl_3]$ ($M = V, Cr$) and $[M(PNP)Cl_2]$ ($M = Cr, Mn$) is reported. Vanadium and manganese PNP pincer complexes are described for the first time. All complexes are characterized by their magnetic moments, elemental analysis, and ESI MS. In addition, some compounds are characterized by X-ray crystallography. In a preliminary study, these complexes catalyze the oxidative homo-coupling of aryl Grignard reagents in the presence of MeI as oxidizing agents to give symmetrical biaryls, but are inactive in Kumada cross-coupling reactions. The reactivity of V(III), Cr(III), Cr(II) and Mn(II) is compared with related Fe(II) and Co (II) complexes of the types $[Fe(PNP-iPr)Cl_2]$, and $[Co(PNP-iPr)Cl_2]$. In all cases, good to excellent isolated yields are obtained. However, since the respective metal chlorides in the absence of PNP ligands exhibited comparable reactivities, the new PNP complexes offer no real advantage for this type of coupling reactions.

© 2016 Elsevier B.V. All rights reserved.

1. Introduction

Among the many ligand systems that can be found in the chemical literature pincer ligands play an important role and their complexes have attracted tremendous interest due to their high stability, activity and variability [1]. These tridentate ligands are often planar scaffolds consisting of neutral central pyridine backbone tethered to two, mostly bulky, two-electron donor groups by different spacers. In this family of ligands steric, electronic, and also stereochemical parameters can be manipulated by modifications of the substituents at the donor sites and/or the spacers. Accordingly, many applications of mostly precious second and third row transition metal pincer complexes in the fields of catalysis, molecular recognition and supramolecular chemistry were discovered turning this area into an intensively investigated subject in organometallic chemistry. As non-precious first-row transition metals are concerned, the chemistry of neutral pyridine-based iron [2–7] and cobalt [8,9] PNP complexes experienced an impressive upswing in recent years. Reports on chromium [10], nickel [11,12], and copper [13] PNP pincer complexes are still rare, while vanadium, manganese, and titanium PNP pincer complexes appear to be unknown as yet.

We are currently focusing on the chemistry of non-precious metal complexes containing PNP pincer ligands based on the 2,6-diaminopyridine scaffold, where the pyridine ring and the phosphine moieties are connected via NH, N-alkyl, or N-aryl linkers (Scheme 1) [14].

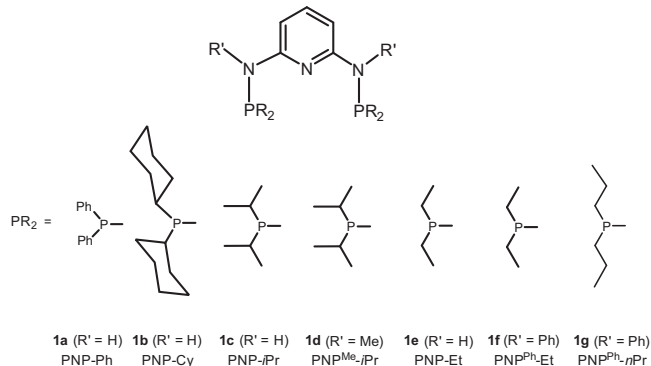
Herein we report on the synthesis, characterization and reactivity of a series of new vanadium, chromium, and manganese PNP complexes of the types $[M(PNP)Cl_3]$ ($M = V, Cr$) and $[M(PNP)Cl_2]$ ($M = Cr, Mn$). In a preliminary study, these complexes were found to catalyze the homo-coupling of PhMgBr in the presence of MeI or atmospheric oxygen as oxidizing agents, but were inactive for cross coupling reactions.

2. Results and discussion

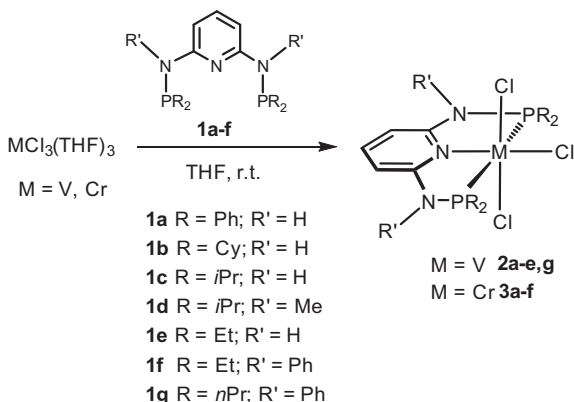
Treatment of $[MCl_3(THF)_3]$ ($M = V, Cr$) with the PNP ligands **1a–g** in THF affords the six-coordinate 14e and 15e complexes $[V(PNP)Cl_3]$ (**2a–e,2g**) and $[Cr(PNP)Cl_3]$ (**3a–f**) in high isolated yields (93–99%), respectively (Scheme 2). Likewise, the reaction of anhydrous MCl_2 ($M = Cr, Mn$) with 1 equiv of the PNP ligands **1a–g** in THF at room temperature afforded the five-coordinate 14e and 15e complexes $[Cr(PNP)Cl_2]$ (**4a–f**) and $[Mn(PNP)Cl_2]$ (**5a–e,5g**) in 92–98% isolated yields (Scheme 3). All complexes display large paramagnetic shifted and very broad 1H NMR signals and thus were not

* Corresponding author.

E-mail address: kkirch@mail.tuwien.ac.at (K. Kirchner).



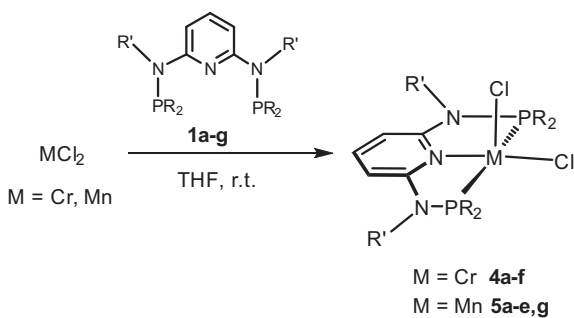
Scheme 1. PNP ligands used in this work (labeling of complexes refers to letters depicted here).



Scheme 2. Synthesis of V(III) and Cr(III) complexes $[\text{V}(\text{PNP})\text{Cl}_3]$ (**2**) and $[\text{Cr}(\text{PNP})\text{Cl}_3]$ (**3**).

very informative. $^{13}\text{C}\{\text{H}\}$ and $^{31}\text{P}\{\text{H}\}$ NMR could not be detected at all. Complexes **2–5** exhibit solution magnetic moments μ_{eff} of 2.7–2.9 μ_{B} , 3.9 μ_{B} , 4.9–5.0 μ_{B} , and 5.9–6.0 μ_{B} (Evans method, in CH_3OH) [15], in agreement with d^2 , d^3 , high spin d^4 , and high spin d^5 electron configurations, respectively.

In order to unequivocally establish the ligand arrangement around the metal centers, the solid state structure of complexes $[\text{V}(\text{PNP-Ph})\text{Cl}_3]$ (**2a**), $[\text{V}(\text{PNP}^{\text{Ph}}-\text{nPr})\text{Cl}_3]$ (**2g**), $[\text{Cr}(\text{PNP-}i\text{Pr})\text{Cl}_3]$ (**3d**), $[\text{Cr}(\text{PNP}^{\text{Me}}-\text{iPr})\text{Cl}_2]$ (**4d**), and $[\text{Mn}(\text{PNP-}i\text{Pr})\text{Cl}_2]$ (**5c**) was determined by X-ray diffraction. Representations of these molecules are shown in Figs. 1–5 with selected metrical parameters given in Table 1. The structures of **2a**, **2g** and **3d** show a distorted-octahedral trivalent vanadium and chromium center surrounded by three meridionally placed donor atoms of the PNP ligand. The three chlorine atoms



Scheme 3. Synthesis of Cr(II) and Mn(II) complexes $[\text{Cr}(\text{PNP})\text{Cl}_2]$ (**4**) and $[\text{Mn}(\text{PNP})\text{Cl}_2]$ (**5**).

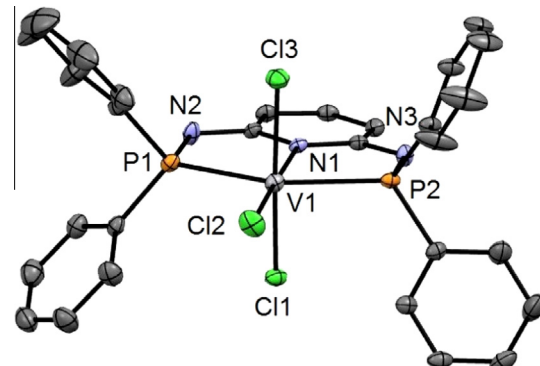


Fig. 1. Structural view of $[\text{V}(\text{PNP-Ph})\text{Cl}_3] \cdot 3.5(\text{CH}_3)_2\text{CO}$ (**2a**·3.5(CH_3)₂CO) showing 50% displacement ellipsoids (H atoms and solvent molecules omitted for clarity).

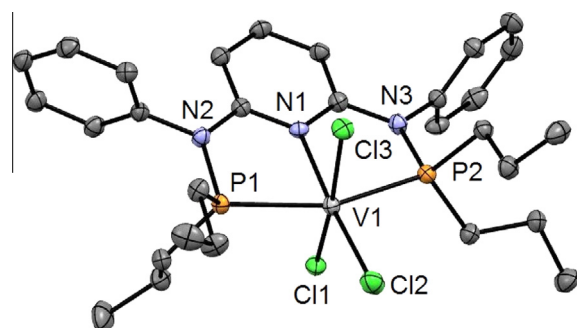


Fig. 2. Structural view of $[\text{V}(\text{PNP}^{\text{Ph}}-\text{nPr})\text{Cl}_3]$ (**2g**) showing 50% displacement ellipsoids (H atoms omitted for clarity).

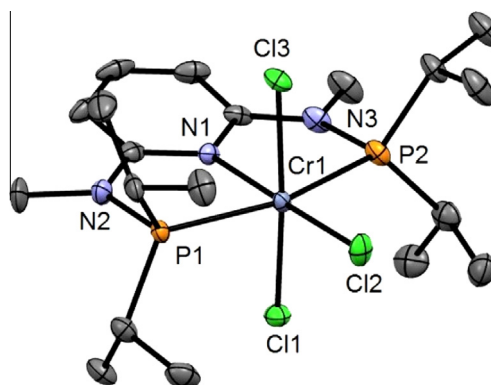


Fig. 3. Structural view of $[\text{Cr}(\text{PNP}^{\text{Me}}-\text{iPr})\text{Cl}_3]$ (**3d**) showing 50% displacement ellipsoids (H atoms and a second independent complex are omitted for clarity).

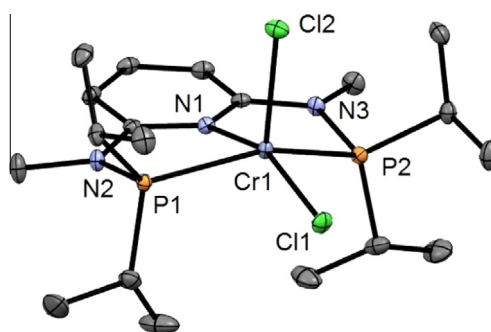


Fig. 4. Structural view of $[\text{Cr}(\text{PNP}^{\text{Me}}-\text{iPr})\text{Cl}_2] \cdot 0.5\text{CH}_2\text{Cl}_2$ (**4d**·0.5 CH_2Cl_2) showing 50% displacement ellipsoids (H atoms and solvent molecules omitted for clarity).

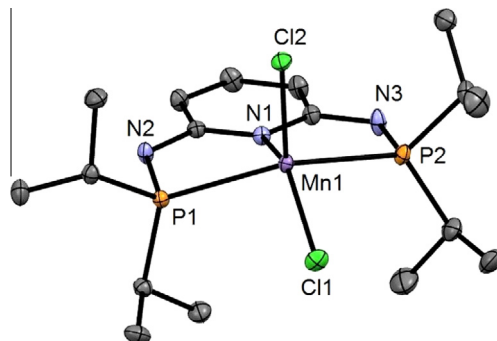


Fig. 5. Structural view of $[\text{Mn}(\text{PNP-}i\text{Pr})\text{Cl}_2]\cdot\text{THF}$ (**5c**·THF) showing 50% displacement ellipsoids (H atoms and solvent molecules omitted for clarity).

occupy the three remaining positions. In all complexes the Cl1–metal–Cl3 angles deviate from linearity being $165.92(2)^\circ$, $168.13(3)^\circ$, and $172.30(3)^\circ$, respectively, and are contracted towards the pyridine ring. The same pattern is observed for the P1–metal–P2 angles which are $156.25(2)^\circ$, $158.38(3)^\circ$, and $162.41(3)^\circ$, respectively. The coordination geometry of the metal center in **4d** and **5c** is distorted square pyramidal with the chromium and manganese atoms lying $0.463(1)$ and $0.416(1)\text{\AA}$ out of the pyridine plane. For comparison, in $[\text{Fe}(\text{PNP-}i\text{Pr})\text{Cl}_2]$ [14b] and $[\text{Fe}(\text{PNP}^{\text{Me}}\text{-}i\text{Pr})\text{Cl}_2]$ [14k] these values are $0.288(1)$ and $0.708(1)\text{\AA}$. The Cr–Cl1 (basal) bond length is significantly shorter ($2.3381(5)\text{\AA}$) than the distance to the apical chlorine (Cr–Cl2 $2.4684(5)\text{\AA}$). This order is reversed in **5c**, where the Mn–Cl1 (basal) bond length is slightly longer ($2.3940(5)\text{\AA}$) than the Mn–Cl2 distance being $2.3658(5)\text{\AA}$ as well as for $[\text{Fe}(\text{PNP}^{\text{Me}}\text{-}i\text{Pr})\text{Cl}_2]$ ($2.347(1)$ versus $2.301(1)\text{\AA}$) and $[\text{Fe}(\text{PNP-}i\text{Pr})\text{Cl}_2]$ ($2.3708(7)$ versus $2.3040(6)\text{\AA}$) (Table 1). Thus, the metal–Cl2 (apical) bond distance is most sensitive to the nature of the metal decreasing in the order Cr(II) > Mn(II) > Fe(II) > Co(II).

Since ESI-MS enables not only the detection and the study of reaction substrates and products but also short-lived reaction intermediates and decomposition products as they are present in solution, representative PNP complexes were investigated by means of this technique. Methanol solutions of $[\text{V}(\text{PNP}^{\text{Me}}\text{-}i\text{Pr})\text{Cl}_3]$ (**2d**), $[\text{Cr}(\text{PNP-}i\text{Pr})\text{Cl}_3]$ (**3c**), $[\text{Cr}(\text{PNP}^{\text{Me}}\text{-}i\text{Pr})\text{Cl}_2]$ (**4d**), $[\text{Mn}(\text{PNP-}i\text{Pr})\text{Cl}_2]$ (**5c**), and, for comparison, $[\text{Fe}(\text{PNP-}i\text{Pr})\text{Cl}_2]$ and $[\text{Co}(\text{PNP-}i\text{Pr})\text{Cl}_2]$ in the presence of NaCl were subjected to ESI-MS analysis in the positive ion mode. The full scan ESI-MS spectra are depicted in Fig. 6 (spectra A – F).

In the case of the V(III) complex **2d**, the most abundant signal at m/z 443.1 corresponds to an oxidized mono chloro V(IV) species bearing an oxo ligand $[\text{M}(\text{V}^{4+})+\text{O}-2\text{Cl}]^+$ emphasizing the sensitivity of this complex towards oxygen (spectrum A). It has to be noted that, even though solutions are prepared under an argon

atmosphere, traces of oxygen in the mass spectrometer are unavoidable. For the Cr(III) complex **3c** the sodiated complex $[\text{M}(\text{Cr}^{3+})+\text{Na}]^+$ and also $[\text{M}(\text{Cr}^{3+})-\text{Cl}]^+$, where one chloride ligand is lost, were found as the main fragment ions in the full mass spectrum at m/z 521.1 and 463.1, respectively, (spectrum B).

In the divalent M(II) series, the various fragments are shown in Scheme 4. The Cr(II) complex **4d** undergoes oxidation to form Cr(III) complexes (spectrum C). Signals of the formal NaCl adduct $[\text{M}(\text{Cr}^{3+})+\text{NaCl}]^+$ and $[\text{M}(\text{Cr}^{3+})-\text{Cl}]^+$ are detected at m/z 549.1 and 491.1, respectively. In the case of Mn(II), the fully intact but sodiated complex $[\text{M}(\text{Mn}^{2+})+\text{Na}]^+$ was observed at m/z 489.1 (spectrum D). Both Fe(II) and Co(II) complexes $[\text{Fe}(\text{PNP-}i\text{Pr})\text{Cl}_2]$ and $[\text{Co}(\text{PNP-}i\text{Pr})\text{Cl}_2]$ lose one chloride ligand giving rise to the cationic fragments $[\text{M}(\text{Fe}^{2+})-\text{Cl}]^+$ and $[\text{M}(\text{Co}^{2+})-\text{Cl}]^+$ at m/z 432.1 and 435.1 (spectra E, F). In addition, the iron complex forms a methanol adduct $[\text{M}(\text{Fe}^{2+})+\text{CH}_3\text{OH}-\text{Cl}]^+$ (m/z 464.1) revealing the high affinity of CH_3OH towards Fe(II) complexes. Similar observations were made recently with Fe(II) PNP pincer complexes based on *R,R*-TADDOL in combination with bulky *i*Pr and *t*Bu substituents [14i].

Having a series of well-defined V(III), Cr(III), Cr(II), and Mn(II) PNP complexes in hands, we decided to investigate their catalytic activity in the Kumada cross-coupling of PhMgBr and aryl halides. Unfortunately, no cross coupling took place and only homo-coupling product (biphenyl) was obtained. Thus, complexes **2a–c**, **3c**, **4a–d**, and **5c** as well as $[\text{Fe}(\text{PNP-}i\text{Pr})\text{Cl}_2]$, and $[\text{Co}(\text{PNP-}i\text{Pr})\text{Cl}_2]$ were reacted with PhMgBr in the presence of MeI in THF as solvent at room temperature. For comparison, also the chloride salts of V(III), Cr(III), Cr(II), Mn(II), Fe(II) and Co(II) in the absence of PNP ligands were tested as catalysts. This reaction constitutes an easy and efficient method to obtain symmetrical biaryl compounds. In recent years, several non-precious metal complexes were found to catalyze this reaction including manganese [16,17] and iron complexes [17,18]. As oxidants typically 1,2-dichloroethane or atmospheric oxygen are used. As shown in Table 2, excellent isolated yields (62–93%) of biphenyl were obtained by using 0.1 mol % of catalyst with very short reaction times (15 min with MeI and 45 min in the presence of dry air). Yields up to 93% were achieved with Cr(II) PNP complexes and MeI. It has to be noted that all reactions with MeI proceed with gas evolution presumably due to the formation of ethane. The reactions with the chloride salts were less efficient in the case of V(III), Cr(III), and Mn(II), but only slightly worse with Cr(II), Fe(II), and Co(II) chlorides. Accordingly, the new PNP complexes offer no real advantage for homo coupling reactions.

$[\text{Cr}(\text{PNP-}i\text{Pr})\text{Cl}_2]$ (**4c**) was also tested as catalyst for the oxidative homo-coupling of several aryl magnesium bromides and PhMgCl with MeI as oxidant. The results of this study are presented in Table 3. With **4c** and aryl magnesium bromides excellent yields of symmetrical biaryls were obtained (entries 1 and 3–6, 62–91%). Also with PhMgCl biphenyl was formed in high yields but required a slightly longer reaction time (entry 2).

Table 1

Selected bond distances and angles (U+00C5, °) of the square pyramidal high-spin Cr(II), Mn(II), Fe(II), and Co(II) complexes $[\text{Cr}(\text{PNP}^{\text{Me}}\text{-}i\text{Pr})\text{Cl}_2]$ (**4d**), $[\text{Mn}(\text{PNP-}i\text{Pr})\text{Cl}_2]$ (**5c**), $[\text{Fe}(\text{PNP-}i\text{Pr})\text{Cl}_2]$ [14b], $[\text{Fe}(\text{PNP}^{\text{Me}}\text{-}i\text{Pr})\text{Cl}_2]$ [14k], and $[\text{Co}(\text{PNP-}i\text{Pr})\text{Cl}_2]$ [2c].

	4d	5c	$[\text{Fe}(\text{PNP-}i\text{Pr})\text{Cl}_2]$	$[\text{Fe}(\text{PNP}^{\text{Me}}\text{-}i\text{Pr})\text{Cl}_2]$	$[\text{Co}(\text{PNP-}i\text{Pr})\text{Cl}_2]$
M–Cl1 (basal)	2.3381(5)	2.3940(5)	2.3708(7)	2.347(1)	2.247(2)
M–Cl2 (apical)	2.4684(5)	2.3658(5)	2.3040(6)	2.301(1)	2.279(2)
M–N1	2.1270(9)	2.356(5)	2.250(2)	2.290(3)	2.097(5)
M–P1	2.4257(5)	2.5931(5)	2.4631(7)	2.464(1)	2.550(2)
M–P2	2.4301(5)	2.5794(5)	2.4844(7)	2.443(1)	2.542(2)
Cl1–M–Cl2	101.10(1)	113.19(2)	107.60(3)	106.71(4)	117.68(8)
P1–M–P2	148.31(2)	142.16(1)	146.56(3)	140.89(4)	155.36(6)
N1–M–Cl2	157.10(3)	139.71(1)	144.13(6)	145.45(8)	130.4(2)

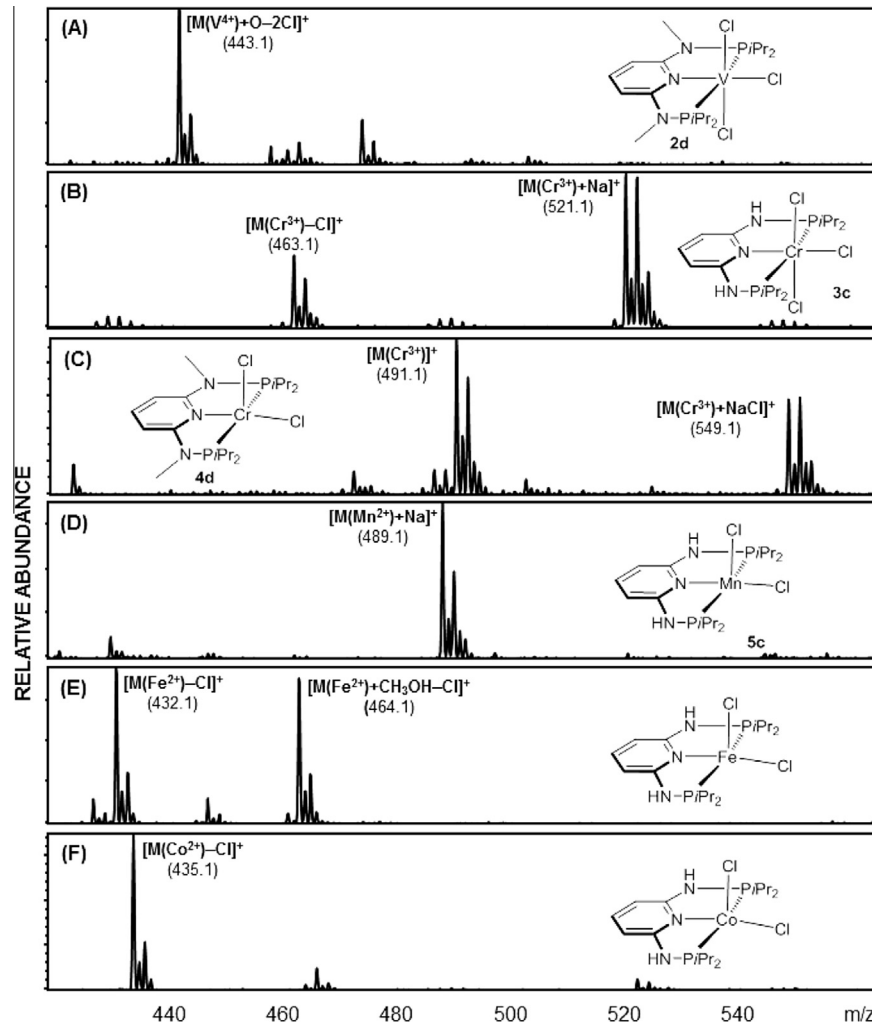


Fig. 6. Positive-ion ESI full scan mass spectra of complexes **2d**, **3c**, **4d**, **5c**, $[Fe(PNP-iPr)Cl_2]$, and $[Co(PNP-iPr)Cl_2]$. All mass calculations and mass assignments are based on the most abundant metal isotope (^{51}V , ^{52}Cr , ^{55}Mn , ^{56}Fe , ^{59}Co -isotopes) and the Cl isotope of lowest mass (^{35}Cl).

3. Conclusion

In sum, we describe here the synthesis of a series of vanadium, chromium, and manganese PNP complexes of the types $[M(PNP)Cl_3]$ ($M = V, Cr$) and $[M(PNP)Cl_2]$ ($M = Cr, Mn$). Vanadium and manganese PNP pincer complexes were as yet not reported. All complexes are characterized by their magnetic moments, elemental analysis and ESI MS. In addition, some compounds were characterized by X-ray crystallography. In a preliminary study, these complexes catalyze the oxidative homo-coupling of aryl Grignard reagents in the presence of MeI as oxidizing agents to give symmetrical biaryls, but are inactive in Kumada cross-coupling reactions. The reactivity of V(III), Cr(III), Cr(II) and Mn(II) is compared with related Fe(II) and Co(II) complexes of the types $[Fe(PNP-iPr)Cl_2]$, and $[Co(PNP-iPr)Cl_2]$. In all cases, good to excellent isolated yields are obtained. However, since the respective metal chlorides in the absence of PNP ligands exhibited comparable reactivities, the new PNP complexes offer no real advantage for this type of coupling reactions.

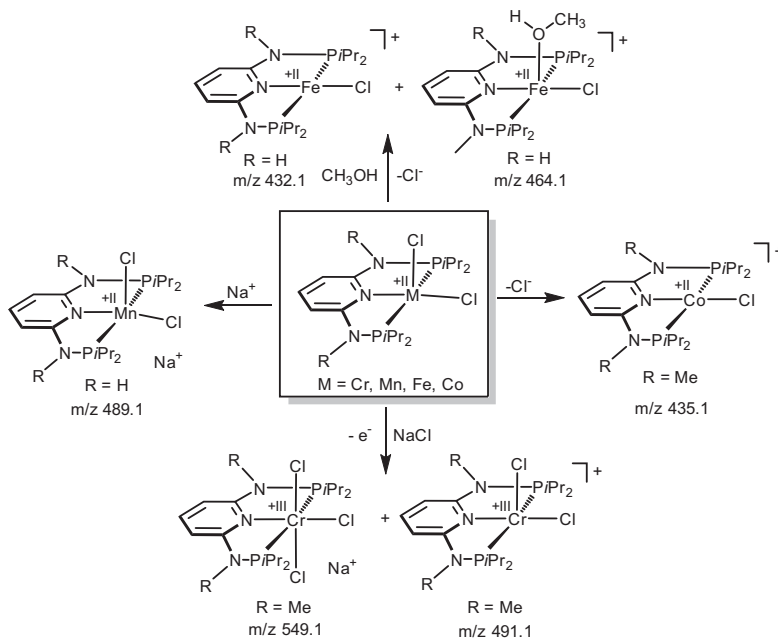
4. Experimental

4.1. General

All manipulations were performed under an inert atmosphere of argon by using Schlenk techniques or in an MBraun inert-gas

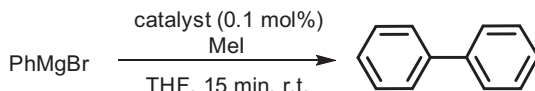
glovebox. The solvents were purified according to standard procedures [19]. The deuterated solvents were purchased from Aldrich and dried over 4 Å molecular sieves. The ligands N,N'-bis(diphenylphosphino)-2,6-diaminopyridine (PNP-Ph) (**1a**) [10a] N, N'-bis(dicyclohexyl)-2,6-diaminopyridine (PNP-Cy) (**1b**) [14k] N, N'-bis(diisopropylphosphino)-2,6-diaminopyridine (PNP-iPr) (**1c**) [14a], N,N'-bis(diisopropylphosphino)-N,N'-dimethyl-2,6-diaminopyridine (PNP^{Me}-iPr) (**1d**) [20], N,N'-bis(diethylphosphino)-2,6-diaminopyridine (PNP-Et) (**1e**), N,N'-bis(ethylphosphino)-N, N'-diphenyl-2,6-diaminopyridine (PNP^{Ph}-Et) (**1f**), and N,N'-bis(*n*-propylphosphino)-N,N'-diphenyl-2,6-diaminopyridine (PNP^{Ph}-*n*Pr) (**1g**) [14h] and complexes $[Fe(PNP-iPr)Cl_2]$ [**14b**], and $[Co(PNP-iPr)Cl_2]$ [**8d**] were prepared according to the literature. 1H , ^{13}C { 1H }, and ^{31}P { 1H } NMR spectra were recorded on Bruker AVANCE-250, AVANCE-300 DPX, and AVANCE-400 spectrometers. 1H and ^{13}C { 1H } NMR spectra were referenced internally to residual protio-solvent, and solvent resonances, respectively, and are reported relative to tetramethylsilane ($\delta = 0$ ppm). ^{31}P { 1H } NMR spectra were referenced externally to H_3PO_4 (85%) ($\delta = 0$ ppm). Room-temperature solution (CH_3OH) magnetic moments were determined by 1H NMR spectroscopy using the method of Evans [15].

All mass spectrometric measurements were performed on an Esquire 3000^{plus} 3D-quadrupole ion trap mass spectrometer (Bruker Daltonics, Bremen, Germany) in positive-ion mode by means of electrospray ionization (ESI). Mass calibration was done with a



Scheme 4. Fragmentation pathways of M(II) complexes $[M(\text{PNP}^{\text{R}}\text{-iPr})\text{Cl}_2]$ ($M = \text{Cr}, \text{Mn}, \text{Fe}, \text{Co}; \text{R} = \text{H} \text{ or } \text{Me}$) in CH_3OH in the presence of NaCl as established by ESI MS experiments.

Table 2
Catalyst screening in the homo-coupling of PhMgBr with MeI^{a} as oxidizing agents.



Oxidation state	Catalyst	Additive	t (min)	Yield ^b (%)
V(III)	$\text{V}(\text{PNP-Ph})\text{Cl}_3$ (2a)	MeI	15	81
V(III)	$\text{V}(\text{PNP-iPr})\text{Cl}_3$ (2c)	MeI	15	85
V(III)	$\text{V}(\text{PNP}^{\text{Me}}\text{-iPr})\text{Cl}_3$ (2d)	MeI	15	85
V(III)	VCl_3	MeI	15	59
Cr(III)	$\text{Cr}(\text{PNP-iPr})\text{Cl}_3$ (3c)	MeI	15	82
Cr(III)	CrCl_3	MeI	15	33
Cr(II), h. s. ^c	$\text{Cr}(\text{PNP-Ph})\text{Cl}_2$ (4a)	MeI	15	89
Cr(II), h. s.	$\text{Cr}(\text{PNP-Cy})\text{Cl}_2$ (4b)	MeI	15	92
Cr(II), h. s.	$\text{Cr}(\text{PNP}^{\text{Me}}\text{-iPr})\text{Cl}_2$ (4c)	MeI	15	91
Cr(II), h. s.	$\text{Cr}(\text{PNP}^{\text{Me}}\text{-iPr})\text{Cl}_2$ (4d)	MeI	15	93
Cr(II), h. s.	CrCl_2	MeI	15	73
Mn(II), h. s.	$\text{Mn}(\text{PNP-iPr})\text{Cl}_2$ (5c)	MeI	15	81
Mn(II), h. s.	MnCl_2	MeI	15	38
Fe(II), h. s.	$\text{Fe}(\text{PNP-iPr})\text{Cl}_2$	MeI	15	73
Fe(II), h. s.	FeCl_2	MeI	15	69
Co(II), h. s.	$\text{Co}(\text{PNP-iPr})\text{Cl}_2$	MeI	15	88
Co(II), h. s.	CoCl_2	MeI	15	71

^a The reactions were carried out using PhMgBr (10.5 mmol), MeI (10.0 mmol), and catalyst (0.01 mmol) in THF (8.5 mL).

^b Isolated yields after column chromatography.

^c h. s. = high spin.

commercial mixture of perfluorinated trialkyl-triazines (ES Tuning Mix, Agilent Technologies, Santa Clara, CA, USA). All analytes were dissolved in methanol “hypergrade for LC–MS Lichrosolv” quality (Merck, Darmstadt, Germany) to form a concentration of roughly 1 mg/mL and doped with sodium chloride to suppress dissociation of chloride ligands from the metal complexes and/or to promote the corresponding $[\text{M}+\text{Na}]^+$ or $[\text{M}+\text{NaCl}]^+$ (formally added by oxidation of the central metal cation by a one electron oxidation step)

ion formation. Direct infusion experiments were carried out using a Cole Parmer model 74900 syringe pump (Cole Parmer Instruments, Vernon Hills, IL, USA) at a flow rate of 2 $\mu\text{L}/\text{min}$. Full scan and MS/MS (low energy CID)-scans were measured in the range m/z 100–1100 with the target mass set to m/z 1000. Further experimental conditions include: drying gas temperature: 150 °C; capillary voltage: -4 kV; skimmer voltage: 40 V; octapole and lens voltages: according to the target mass set. All mass calculations are based on the most abundant metal isotopes (^{50}V , ^{52}Cr , ^{55}Mn , ^{56}Fe , ^{59}Co -isotopes) and the Cl isotope of lowest mass (^{35}Cl). Mass spectra were averaged during data acquisition time of 1–2 min and one analytical scan consisted of five successive micro scans resulting in 50 and 100 analytical scans, respectively, for the final full scan mass spectrum.

4.2. Synthesis

4.2.1. $[\text{CrCl}_3(\text{THF})_3]$

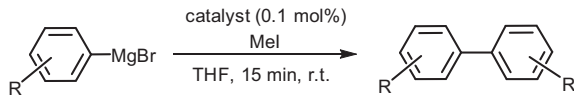
Anhydrous CrCl_3 (20 g, 126.3 mmol) and Zn powder (200 mg, 3.05 mmol) were mixed in a glass frit and extracted with dry THF (400 mL) in a Soxhlet extractor under inert conditions for 48 h. The extracted suspension was reduced to 100 mL, the purple powder was collected by filtration and dried under reduced pressure. Yield: 33.5 g (89%) [21].

4.2.2. $[\text{V}(\text{PNP-Ph})\text{Cl}_3]$ (**2a**)

A suspension of PNP-Ph (**1a**) (477 mg, 1.0 mmol) and VCl_3 (-THF)₃ (374 mg, 1.0 mmol) in THF (15 mL) was stirred for 3 h. The suspension was then reduced to 4 mL and *n*-hexane (15 mL) was added for precipitation. The solid was collected on a glass frit as a brown powder, washed with *n*-hexane, and dried under reduced pressure. Yield: 628 mg (99%). Anal. Calc. for $\text{C}_{29}\text{H}_{25}\text{Cl}_3\text{N}_3\text{P}_2\text{V}$ (634.78): C, 54.87; H, 3.97; N, 6.62. Found: C, 54.95; H, 4.06; N, 6.54%. $\mu_{\text{eff}} = 2.7 \mu\text{B}$.

4.2.3. $[\text{V}(\text{PNP-Cy})\text{Cl}_3]$ (**2b**)

This complex was prepared analogously to **2a** using PNP-Cy (**1b**) (502 mg, 1.0 mmol) and $\text{VCl}_3(\text{THF})_3$ (374 mg, 1.0 mmol) as

Table 3Homo-coupling of aryl magnesium halides with MeI as oxidizing agents utilizing $[\text{Cr}(\text{PNP-iPr})\text{Cl}_2]$ (**4c**) as catalysts.^a

Entry	Catalyst	RMgX	Product	Additive	t (min)	Yield ^b (%)
1	$\text{Cr}(\text{PNP-iPr})\text{Cl}_2$			MeI	15	91
2				MeI	30	79
3				MeI	15	91
4				MeI	15	65
5				MeI	15	62
6				MeI	15	83

^a The reactions were carried out using ArMgX (10.5 mmol), MeI (10.0 mmol), and catalyst (0.01 mmol) in THF (8.5 mL).^b Isolated yields after column chromatography.

starting materials. Yield: 633 mg (96%). *Anal.* Calc. for $\text{C}_{29}\text{H}_{49}\text{Cl}_3\text{N}_3\text{P}_2\text{V}$ (658.97): C, 52.86; H, 7.49; N, 6.38. Found: 52.92; H, 7.55; N, 6.31%. $\mu_{\text{eff}} = 2.7 \mu_B$.

4.2.4. $[\text{V}(\text{PNP-iPr})\text{Cl}_3]$ (**2c**)

This complex was prepared analogously to **2a** using PNP-iPr (**1c**) (341 mg, 1.0 mmol) and $\text{VCl}_3(\text{THF})_3$ (374 mg, 1.0 mmol) as starting materials. Yield: 450 mg (95%). *Anal.* Calc. for $\text{C}_{17}\text{H}_{33}\text{Cl}_3\text{N}_3\text{P}_2\text{V}$ (498.71): C, 40.94; H, 6.67; N, 8.43. Found: C, 41.10; H, 6.68; N, 8.52%. $\mu_{\text{eff}} = 2.7 \mu_B$.

4.2.5. $[\text{V}(\text{PNP}^{\text{Me}}\text{-iPr})\text{Cl}_3]$ (**2d**)

This complex was prepared analogously to **2a** using PNP^{Me}-iPr (**1d**) (370 mg, 1.0 mmol) and $\text{VCl}_3(\text{THF})_3$ (374 mg, 1.0 mmol) as starting materials. Yield: 511 mg (97%). *Anal.* Calc. for $\text{C}_{19}\text{H}_{37}\text{Cl}_3\text{N}_3\text{P}_2\text{V}$ (526.77): C, 43.32; H, 7.08; N, 7.98. Found: C, 43.34; H, 7.09; N, 7.97. $\mu_{\text{eff}} = 2.7 \mu_B$.

4.2.6. $[\text{V}(\text{PNP-Et})\text{Cl}_3]$ (**2e**)

This complex was prepared analogously to **2a** using PNP-Et (**1e**) (285 mg, 1.0 mmol) and $\text{VCl}_3(\text{THF})_3$ (374 mg, 1.0 mmol) as starting materials. Yield: 438 mg (99%). *Anal.* Calc. for $\text{C}_{13}\text{H}_{25}\text{Cl}_3\text{N}_3\text{P}_2\text{V}$ (442.61): C, 35.28; H, 5.69; N, 9.49. Found: C, 35.31; H, 5.68; N, 9.51%. $\mu_{\text{eff}} = 2.8 \mu_B$.

4.2.7. $[\text{V}(\text{PNP}^{\text{Ph}}\text{-Pr})\text{Cl}_3]$ (**2g**)

This complex was prepared analogously to **2a** using PNP^{Ph}-nPr (**1g**) (494 mg, 1.0 mmol) and $\text{VCl}_3(\text{THF})_3$ (374 mg, 1.0 mmol) as starting materials. Yield: 631 mg (97%). *Anal.* Calc. for $\text{C}_{29}\text{H}_{41}\text{Cl}_3\text{N}_3\text{P}_2\text{V}$ (650.90): C, 53.51; H, 6.35; N, 6.46. Found: 53.48; H, 6.32; N, 6.49%. $\mu_{\text{eff}} = 2.8 \mu_B$.

4.2.8. $[\text{Cr}(\text{PNP-Ph})\text{Cl}_3]$ (**3a**)

A solution of PNP-Ph (**1a**) (477 mg, 1.0 mmol) and $\text{CrCl}_3(\text{THF})_3$ (374 mg, 1.0 mmol) in THF (10 mL) was stirred for 16 h at 50 °C. The purple solution was then reduced to 2 mL and *n*-hexane (10 mL) was added for precipitation. The purple powder was collected on a glass frit, washed with *n*-hexane, dried under vacuum. Yield: 616 mg (97%). *Anal.* Calc. for $\text{C}_{29}\text{H}_{25}\text{Cl}_3\text{CrN}_3\text{P}_2$ (635.83): C, 54.76; H, 3.95; N, 6.60. Found: C, 54.65; H, 3.89; N, 6.70%. $\mu_{\text{eff}} = 3.9 \mu_B$.

4.2.9. $[\text{Cr}(\text{PNP-Cy})\text{Cl}_3]$ (**3b**)

This complex was prepared analogously to **3a** using PNP-Cy (**1b**) (501 mg, 1.0 mmol) and $\text{CrCl}_3(\text{THF})_3$ (374 mg, 1.0 mmol). Yield: 620 mg (94%). *Anal.* Calc. for $\text{C}_{29}\text{H}_{49}\text{Cl}_3\text{CrN}_3\text{P}_2$ (660.03): C, 52.77; H, 7.48; N, 6.36. Found: C, 52.83; H, 7.65; N, 6.21%. $\mu_{\text{eff}} = 3.9 \mu_B$.

4.2.10. $[\text{Cr}(\text{PNP-iPr})\text{Cl}_3]$ (**3c**)

This complex was prepared analogously to **3a** using PNP-iPr (**1c**) (341 mg, 1.0 mmol) and $\text{CrCl}_3(\text{THF})_3$ (374 mg, 1.0 mmol). Yield: 464 mg (93%). *Anal.* Calc. for $\text{C}_{17}\text{H}_{33}\text{Cl}_3\text{CrN}_3\text{P}_2$ (499.77): C, 40.85; H, 6.65; N, 8.41. Found: C, 40.85; H, 6.65; N, 8.41%. $\mu_{\text{eff}} = 3.9 \mu_B$.

4.2.11. $[\text{Cr}(\text{PNP}^{\text{Me}}\text{-iPr})\text{Cl}_3]$ (**3d**)

This complex was prepared analogously to **3a** using PNP^{Me}-iPr (**1d**) (369 mg, 1.0 mmol) and $\text{CrCl}_3(\text{THF})_3$ (374 mg, 1.0 mmol) as starting materials. Yield: 506 mg (96%). *Anal.* Calc. for $\text{C}_{19}\text{H}_{37}\text{Cl}_3\text{CrN}_3\text{P}_2$ (527.82): C, 43.23; H, 7.07; N, 7.95. Found: C, 43.15; H, 7.15; N, 8.00%. $\mu_{\text{eff}} = 3.9 \mu_B$.

4.2.12. $[Cr(PNP^{Ph}-Et)Cl_3]$ (**3f**)

This complex was prepared analogously to **3a** using PNP^{Ph}-Et (**1f**) (437 mg, 1.0 mmol) and CrCl₃(THF)₃ (374 mg, 1.0 mmol) as starting materials. Yield: 567 mg (93%). *Anal.* Calc. for C₂₅H₃₃Cl₂CrN₃P₂ (595.84): C, 50.37; H, 5.57; N, 7.04. Found: C, 50.15; H, 5.45; N, 7.11%. μ_{eff} = 3.9 μ_B .

4.2.13. $[Cr(PNP-Ph)Cl_2]$ (**4a**)

A solution of PNP-Ph (**1a**) (477 mg, 1.0 mmol) and CrCl₂ (122 mg, 1.0 mmol) in THF (10 mL) was stirred for 16 h. The green solution was reduced to 2 mL and *n*-hexane (10 mL) was added for precipitation. The dark green powder was collected on a glass frit, and dried under reduced pressure. Yield: 557 mg (95%). *Anal.* Calc. for C₂₉H₂₅Cl₂CrN₃P₂ (600.38): C, 58.01; H, 4.19; N, 7.00. Found: C, 58.15; H, 4.15; N, 6.91%. μ_{eff} = 5.0 μ_B .

4.2.14. $[Cr(PNP-Cy)Cl_2]$ (**4b**)

This complex was prepared analogously to **4a** using PNP-Cy (**1b**) (501 mg, 1.0 mmol) and CrCl₂ (122 mg, 1.0 mmol) as starting materials. Yield: 607 mg (97%). *Anal.* Calc. for C₂₉H₄₉Cl₂CrN₃P₂ (624.58): C, 55.77; H, 7.90; N, 6.72. Found: C, 55.85; H, 7.65; N, 6.82%. μ_{eff} = 5.0 μ_B .

4.2.15. $[Cr(PNP-iPr)Cl_2]$ (**4c**)

This complex was prepared analogously to **4a** using PNP-iPr (**1c**) (341 mg, 1.0 mmol) and CrCl₂ (122 mg, 1.0 mmol) as starting materials. Yield: 441 mg (95%). *Anal.* Calc. for C₁₇H₃₃Cl₂CrN₃P₂ (464.32): C, 43.91; H, 7.14; N, 9.04. Found: C, 43.99; H, 7.25; N, 9.11%. μ_{eff} = 5.0 μ_B .

4.2.16. $[Cr(PNP^{Me}-iPr)Cl_2]$ (**4d**)

This complex was prepared analogously to **4a** using PNP^{Me}-iPr (**1d**) (369 mg, 1.0 mmol) and CrCl₂ (122 mg, 1.0 mmol) as starting materials. Yield: 472 mg (96%). *Anal.* Calc. for C₁₉H₃₇Cl₂CrN₃P₂ (492.37): C, 46.34; H, 7.56; N, 8.52. Found: C, 46.25; H, 7.61; N, 8.62%. μ_{eff} = 5.0 μ_B .

4.2.17. $[Cr(PNP^{Ph}-Et)Cl_2]$ (**4f**)

This complex was prepared analogously to **4a** using PNP^{Ph}-Et (**1f**) (437 mg, 1.0 mmol) and CrCl₂ (122 mg, 1.0 mmol) as starting materials. Yield: 515 mg (92%). *Anal.* Calc. for C₂₅H₃₃Cl₂CrN₃P₂ (560.40): C, 53.57; H, 5.94; N, 7.49. Found: C, 53.65; H, 5.85; N, 7.44%. μ_{eff} = 5.0 μ_B .

4.2.18. $[Mn(PNP-Ph)Cl_2]$ (**5a**)

PNP-Ph (**1a**) (477 mg, 1.0 mmol) and anhydrous MnCl₂ (126 mg, 1.0 mmol) were suspended in THF (10 mL) and stirred for 16 h. The suspension was reduced to 4 mL and *n*-hexane (20 mL) was added for precipitation. The off-white powder was collected by filtration and dried under reduced pressure. Yield: 579 mg (96%). *Anal.* Calc. for C₂₉H₂₅Cl₂MnN₃P₂ (603.32): C, 57.73; H, 4.18; N, 6.96. Found: C, 57.71; H, 4.17; N, 6.94%. μ_{eff} = 6.0 μ_B .

4.2.19. $[Mn(PNP-Cy)Cl_2]$ (**5b**)

This complex was prepared analogously to **5a** using PNP-Cy (**1b**) (501 mg, 1.0 mmol) and anhydrous MnCl₂ (126 mg, 1.0 mmol) as starting materials. Yield: 596 mg (95%). *Anal.* Calc. for C₂₉H₄₉Cl₂MnN₃P₂ (627.51): C, 55.51; H, 7.87; N, 6.70. Found: C, 55.56; H, 7.84; N, 6.74%. μ_{eff} = 5.9 μ_B .

4.2.20. $[Mn(PNP-iPr)Cl_2]$ (**5c**)

This complex was prepared analogously to **5a** using PNP-iPr (**1c**) (341 mg, 1.0 mmol) and anhydrous MnCl₂ (126 mg, 1.0 mmol) as starting materials. Yield: 450 mg (96%). *Anal.* Calc. for C₁₇H₃₃Cl₂MnN₃P₂ (467.26): C, 43.70; H, 7.12; N, 8.99. Found: C, 43.82; H, 7.15; N, 9.05%. μ_{eff} = 6.1 μ_B .

4.2.21. $[Mn(PNP^{Me}-iPr)Cl_2]$ (**5d**)

This complex was prepared analogously to **5a** using PNP^{Me}-iPr (**1d**) (369 mg, 1.0 mmol) and anhydrous MnCl₂ (126 mg, 1.0 mmol) as starting materials. Yield: 466 mg (94%). *Anal.* Calc. for C₁₉H₃₇Cl₂MnN₃P₂ (495.31): C, 46.07; H, 7.53; N, 8.48. Found: C, 46.16; H, 7.59; N, 8.41%. μ_{eff} = 6.0 μ_B .

4.2.22. $[Mn(PNP-Et)Cl_2]$ (**5f**)

This complex was prepared analogously to **5a** using PNP-Et (**1f**) (285 mg, 1.0 mmol) and anhydrous MnCl₂ (126 mg, 1.0 mmol) as starting materials. Yield: 402 mg (98%). *Anal.* Calc. for C₁₃H₂₅Cl₂MnN₃P₂ (411.15): C, 37.98; H, 6.13; N, 10.22. Found: C, 37.89; H, 6.23; N, 10.30%. μ_{eff} = 6.1 μ_B .

4.2.23. $[Mn(PNP^{Ph}-Pr)Cl_2]$ (**5g**)

This complex was prepared analogously to **5a** using PNP^{Ph}-nPr (**1g**) (494 mg, 1.0 mmol) and anhydrous MnCl₂ (126 mg, 1.0 mmol) as starting materials. Yield: 588 mg (95%). *Anal.* Calc. for C₂₉H₄₁Cl₂MnN₃P₂ (619.45): C, 56.23; H, 6.67; N, 6.78. Found: C, 56.18; H, 6.55; N, 6.86%. μ_{eff} = 6.0 μ_B .

4.3. General procedure for the oxidative homocoupling of ArMgBr with MeI

A 3.0 M solution of ArMgBr in Et₂O (3.5 mL, 10.5 mmol) was mixed with 1 mL of a 10 mM stock solution of the catalyst (0.01 mmol) in THF under stirring. A 5 M solution of MeI (2 mL, 10.0 mmol) was added and the mixture was allowed to react for 15 min and was then quenched with iPrOH (0.5 mL). The product was purified by silica column chromatography.

4.4. Crystal structure determination

X-ray diffraction data of **2a**·3.5(CH₃)₂CO, **2g**, **3d**, **4d**·0.5CH₂Cl₂, and **5c**·THF were collected at T = 100 K in a dry stream of nitrogen on a Bruker KAPPA APEX II diffractometer system with graphite monochromatized Mo K α radiation (λ = 0.71073 Å) and fine sliced φ - and ω -scans. Data were reduced to intensity values with SAINT and an absorption correction was applied with the multi-scan approach implemented in SADABS [22]. The structures of **2a**·3.5(CH₃)₂CO, **3d**, **4d**·0.5CH₂Cl₂, and **5c**·THF were solved by charge-flipping implemented in SUPERFLIP [23] and refined using JANA2006 [24] against F. The structure of **2g** was solved with direct methods implemented in SHELXS and refined using SHELXL [25] against F². Non-hydrogen atoms were refined with anisotropic displacement parameters. The H atoms connected to C atoms were placed in calculated positions and thereafter refined as riding on the parent atoms. The H atoms of the amine groups were located in difference Fourier maps. The N-H distances were restrained to 0.870(1) Å in **2a**. In **5c** the H atoms attached to N were freely refined. Molecular graphics were generated with the program MERCURY [26].

Acknowledgements

Financial support by the Austrian Science Fund (FWF) is gratefully acknowledged (Project No. P24583-N28). The X-ray center of the Vienna University of Technology is acknowledged for financial support and for providing access to the single-crystal diffractometer.

Appendix A. Supplementary material

CCDC 1434128–1434132 contains the supplementary crystallographic data for compounds **2a**·3.5(CH₃)₂CO, **2g**, **3d**, **4d**·0.5CH₂Cl₂, and **5c**·THF. These data can be obtained free of charge from The

Cambridge Crystallographic Data Centre via www.ccdc.cam.ac.uk/data_request/cif. Supplementary data associated with this article can be found, in the online version, at <http://dx.doi.org/10.1016/j.ica.2016.02.064>.

References

- [1] For reviews on pincer complexes, see: (a) R.A. Gossage, L.A. van de Kuil, G. van Koten, *Acc. Chem. Res.* 31 (1998) 423;
 (b) M. Albrecht, G. van Koten, *Angew. Chem., Int. Ed.* 40 (2001) 3750;
 (c) M.E. van der Boom, D. Milstein, *Chem. Rev.* 103 (2003) 1759;
 (d) J.T. Singleton, *Tetrahedron* 59 (2003) 1837;
 (e) L.C. Liang, *Coord. Chem. Rev.* 250 (2006) 1152;
 (f) D. Morales-Morales, C.M. Jensen (Eds.), *The Chemistry of Pincer Compounds*, Elsevier, Amsterdam, 2007;
 (g) H. Nishiyama, *Chem. Soc. Rev.* 36 (2007) 1133;
 (h) D. Benito-Garagorri, K. Kirchner, *Acc. Chem. Res.* 41 (2008) 201;
 (i) J. Choi, A.H.R. MacArthur, M. Brookhart, A.S. Goldman, *Chem. Rev.* 111 (2011) 1761;
 (j) N. Selander, K.J. Szabo, *Chem. Rev.* 111 (2011) 2048;
 (k) P. Bhattacharya, H. Guan, *Inorg. Chem.* 32 (2011) 88;
 (l) S. Schneider, J. Meiners, B. Askewold, *Eur. J. Inorg. Chem.* (2012) 412;
 (m) G. van Koten, D. Milstein (Eds.), *Organometallic Pincer Chemistry*, Vol. 40, Springer, Berlin, 2013. Top. Organomet. Chem.;
 (n) K.J. Szabo, O.F. Wendt, *Pincer and Pincer-Type Complexes: Applications in Organic Synthesis and Catalysis*, Wiley-VCH, Germany, 2014;
 (o) H.A. Younus, N. Ahmad, W. Su, F. Verpoort, *Coord. Chem. Rev.* 276 (2014) 112;
 (p) M. Asay, D. Morales-Morales, *Dalton Trans.* 44 (2015) 17432;
 (q) S. Murugesan, K. Kirchner, *Dalton Trans.* 45 (2016) 416.
- [2] (a) W.V. Dahlhoff, S.M. Nelson, *J. Chem. Soc. (A)* (1971) 2184;
 (b) P. Giannoccaro, G. Vasapollo, C.F. Nobile, A. Sacco, *Inorg. Chim. Acta* 61 (1982) 69;
 (c) G. Müller, M. Klinga, M. Leskelä, B. Rieger, Z. *Anorg. Allg. Chem.* 628 (2002) 2839.
- [3] (a) J. Zhang, M. Gandelman, D. Herrman, G. Leitus, L.J.W. Shimon, Y. Ben-David, D. Milstein, *Inorg. Chim. Acta* 359 (2006) 1955;
 (b) R. Langer, G. Leitus, *Angew. Chem., Int. Ed.* 50 (2011) 2120;
 (c) R. Langer, Y. Diskin-Posner, G. Leitus, L.J. Shimon, Y. Ben-David, D. Milstein, *Angew. Chem., Int. Ed.* 50 (2011) 9948;
 (d) R. Langer, M.A. Iron, L. Konstantinovski, Y. Diskin-Posner, G. Leitus, Y. Ben-David, D. Milstein, *Chem. Eur. J.* 18 (2012) 7196;
 (e) T. Zell, B. Butschke, Y. Ben-David, D. Milstein, *Chem. Eur. J.* 19 (2013) 8068;
 (f) T. Zell, Y. Ben-David, D. Milstein, *Angew. Chem., Int. Ed.* 53 (2014) 4685;
 (g) T. Zell, Y. Ben-David, D. Milstein, *Sci. Technol.* 5 (2015) 822.
- [4] S. Mazza, R. Scopelliti, X. Hu, *Organometallics* 34 (2015) 1538.
- [5] R.J. Trovitch, E. Lobkovsky, P.J. Chirik, *Inorg. Chem.* 45 (2006) 7252.
- [6] E.M. Pelczar, T.J. Emge, K. Krogh-Jespersen, A.S. Goldman, *Organometallics* 27 (2008) 5759.
- [7] W.-S. DeRieux, A. Wong, Y. Schrodi, *J. Organomet. Chem.* 772–773 (2014) 60.
- [8] (a) D.W. Shaffer, S.I. Johnson, A.L. Rheingold, J.W. Ziller, W.A. Goddard III, R.J. Nielsen, J.Y. Yang, *Inorg. Chem.* 53 (2014) 13031;
 (b) S.P. Semproni, C. Milsmann, P.J. Chirik, *J. Am. Chem. Soc.* 136 (2014) 9211;
 (c) S.P. Semproni, C.C.H. Atienza, *Chem. Sci.* 5 (2014) 1956;
 (d) J.V. Obligacion, S.P. Semproni, P.J. Chirik, *J. Am. Chem. Soc.* 136 (2014) 4133;
 (e) E. Khaskin, Y. Diskin-Posner, L. Weiner, G. Leitus, *Chem. Commun.* 49 (2013) 2771;
 (f) L. Chen, P. Ai, J. Gu, S. Jie, B.-G. Li, *J. Organomet. Chem.* 716 (2012) 55.
- [9] (a) S. Roesler, J. Obenauf, R. Kempe, *J. Am. Chem. Soc.* 137 (2015) 7998;
 (b) S. Roesler, M. Ertl, T. Irrgang, R. Kempe, *Angew. Chem., Int. Ed.* 54 (2015) 15046.
- [10] (a) W. Schirmer, U. Flörke, H.J. Haupt, Z. *Anorg. Allg. Chem.* 545 (1987) 83;
 (b) A. Alzamly, S. Gambarotta, I. Korobkov, *Organometallics* 32 (2013) 7204;
 (c) A. Alzamly, S. Gambarotta, I. Korobkov, *Organometallics* 33 (2014) 1602;
 (d) M. Mastalir, M. Glatz, S.R.M.M. de Aguiar, B. Stöger, K. Kirchner, *Organometallics* 35 (2016) 229.
- [11] (a) J.I. van der Vlugt, M. Lutz, E.A. Pidko, D. Vogt, A.L. Spek, *Dalton Trans.* (2009) 1016;
 (b) M. Lutz, J.I. van der Vlugt, D. Vogt, A.L. Spek, *Polyhedron* 28 (2009) 2341.
- [12] (a) M. Vogt, O. Rivada-Wheelaghan, M.A. Iron, G. Leitus, Y. Diskin-Posner, L.J. W. Shimon, Y. Ben-David, D. Milstein, *Organometallics* 32 (2013) 300;
 (b) S. Kundu, W. W. Brennessel, W. D. Jones, *Inorg. Chem.* 50 (2011) 9443.
- [13] (a) J.I. van der Vlugt, E.A. Pidko, D. Vogt, M. Lutz, A.L. Spek, *Inorg. Chem.* 48 (2009) 7513;
 (b) J.I. van der Vlugt, E.A. Pidko, R.C. Bauer, Y. Gloaguen, M.K. Rong, M. Lutz, *Chem. Eur. J.* 17 (2011) 3850;
 (c) J.I. van der Vlugt, E.A. Pidko, D. Vogt, M. Lutz, A.L. Spek, A. Meetsma, *Inorg. Chem.* 47 (2008) 4442.
- [14] (a) D. Benito-Garagorri, E. Becker, J. Wiedermann, W. Lackner, M. Pollak, K. Mereiter, J. Kisala, K. Kirchner, *Organometallics* 25 (2006) 1900;
 (b) D. Benito-Garagorri, J. Wiedermann, M. Pollak, K. Mereiter, K. Kirchner, *Organometallics* 26 (2007) 217;
 (c) D. Benito-Garagorri, M. Puchberger, K. Mereiter, K. Kirchner, *Angew. Chem., Int. Ed.* 47 (2008) 9142;
 (d) D. Benito-Garagorri, L.G. Alves, M. Puchberger, K. Mereiter, L.F. Veiros, M.J. Calhorda, M.D. Carvalho, L.P. Ferreira, M. Godinho, K. Kirchner, *Organometallics* 28 (2009) 6902;
 (e) D. Benito-Garagorri, L.G. Alves, L.F. Veiros, C.M. Standfest-Hauser, S. Tanaka, K. Mereiter, K. Kirchner, *Organometallics* 29 (2010) 4923;
 (f) B. Bichler, C. Holzhacker, B. Stöger, M. Puchberger, L.F. Veiros, K. Kirchner, *Organometallics* 32 (2013) 4114;
 (g) M. Bichler, B. Glatz, K. Stöger, L.F. Mereiter, K. Veiros, *Dalton Trans.* 43 (2014) 14517;
 (h) N. Gorgas, B. Stöger, E. Pittenauer, G. Allmaier, L.F. Veiros, K. Kirchner, *Organometallics* 33 (2014) 6905;
 (i) M. Glatz, B. Bichler, M. Mastalir, B. Stöger, K. Mereiter, M. Weil, E. Pittenauer, G. Allmaier, L.F. Veiros, K. Kirchner, *Dalton Trans.* 44 (2015) 281;
 (j) C. Holzhacker, B. Stöger, M.D. Carvalho, L.P. Ferreira, E. Pittenauer, G. Allmaier, L.F. Veiros, S. Realista, A. Gil, M.J. Calhorda, D. Müller, K. Kirchner, *Dalton Trans.* 44 (2015) 13071;
 (k) M. Glatz, C. Holzhacker, B. Bichler, M. Mastalir, B. Stöger, K. Mereiter, M. Weil, L.F. Veiros, N.C. Mösch-Zanetti, K. Kirchner, *Eur. J. Inorg. Chem.* (2015) 5053.
- [15] S.K. Sur, *J. Magn. Reson.* 82 (1989) 169.
- [16] Y. Yuan, *Appl. Organometal. Chem.* 22 (2008) 15.
- [17] G. Cahiez, A. Moyeux, J. Buendia, *J. Am. Chem. Soc.* 129 (2007) 13788.
- [18] (a) G. Cahiez, C. Chaboche, F. Mahuteau-Betzer, M. Ahr, *Org. Lett.* 7 (2005) 1943;
 (b) T. Nagano, T. Hayashi, *Org. Lett.* 7 (2005) 491.
- [19] D.D. Perrin, W.L.F. Armarego, *Purification of Laboratory Chemicals*, 3rd ed., Pergamon, New York, 1988.
- [20] Ö. Öztopcu, C. Holzhacker, M. Puchberger, M. Weil, K. Mereiter, L.F. Veiros, *Organometallics* 32 (2013) 3042.
- [21] A. Vavoulis, T.E. Austin, S.Y. Tyree, *Inorg. Synth.* 6 (1960) 129.
- [22] Bruker Computer Programs: APEX2, SAINT and SADABS, Bruker AXS Inc., Madison, WI, 2012.
- [23] L. Palatinus, G. Chapuis, *J. Appl. Crystallogr.* 40 (2007) 786.
- [24] V. Petříček, M. Dušek, L. Palatinus, Z. Kristallogr. 229 (2014) 345.
- [25] G. Sheldrick, *Acta Crystallogr., Sect. A* 64 (2008) 112.
- [26] C.F. Macrae, P.R. Edgington, P. McCabe, E. Pidcock, G.P. Shields, R. Taylor, M. Towler, J. van de Streek, *J. Appl. Crystallogr.* 39 (2006) 453.